Diagnosis Method for Wind Turbine Doubly Fed Induction Generator under Grid Defects

F. El Hammouchi, L. El Menzhi, A. Saad

***Abstract*— In this paper, we present a method developed for diagnosis defects of doubly-fed induction generator DFIG used in wind turbine. Initially, we focus on modeling of a non-defected wind conversion system based on mathematic model created in Matlab Simulink which is able to present the behavior of the wind turbine. Then, in order to increase wind energy performance, we suggest the use of an indirect vector control stator field orientation.**

Afterwards, we propose a method to diagnose the defects attacking wind turbine generator. This approach is based on frequency spectrum analysis and Lissajous curves of DFIG stator and rotor currents. The DFIG diagnosis defects method is applied to a non-defected generator to have a reliable reference for normal operation of a wind system. However, connected to the grid, wind turbine generator is affected by faults occurring in electrical power networks. For this reason, the proposed diagnosis method is applied also to a defected generator. The resulting Lissajous curves and frequency spectrums are compared to reference data in order to diagnose generator defects type and severity.

The simulations had been realized by Matlab Simulink. These results showed the efficiency of the proposed method.

***Index Terms*— Defects, diagnosis, doubly-fed induction generator, frequency spectrum, Lissajous curve, wind turbine.**

I. INTRODUCTION

Nowadays, in order to satisfy the high energy demand we need to add new capacity to the grid without destroying our environment. So, it was extremely urgent, both from an environmental and economic standpoint, to look for alternative, renewable and clean energies.

It is in this logic that Morocco has committed to this way of exploiting its natural and renewable resources, especially the sun and the wind. His Majesty the King of Morocco noted his country's commitment to generate 42% of its energy needs from renewable sources by 2020 and 52% by 2030 [1].

This work was submitted for review on December 29th 2018.

F. El Hammouchi, National Higher School of Electricity and Mechanic, Hassan II University, Casablanca 8118, Morocco. (E-mail: elhammouchi.fatima@ gmail.com).

L. El Menzhi, National School of Applied Sciences, Abdelmalek Essaadi University, Tangier 9000, Morocco. (E-mail: elmenzhiensa@gmail.com).

A. Saad, National Higher School of Electricity and Mechanic, Hassan II University, Casablanca 8118, Morocco. (E-mail: saad.abdal@gmail.com).

While, Morocco benefits from an enormous wind potential which is completely free, inexhaustible and renewable, the wind energy cost remains high due to the operational and maintenance costs of such a big structure. For these large size wind turbines, the doubly fed induction generator (DFIG) is the most used in the wind turbine variable speed industry [2].

It offers excellent operational and control features that make their integration with power grids easy and effective [3].

In fact, the DFIG is asynchronous machine fed from the stator and rotor. The rotor of DFIG is connected to the grid through the transformer and the voltage source converters "back-to-back": rotor side converter (RSC) and grid side converter (GSC). A capacitor is placed between two converters to reduce the voltage ripples. The RSC controls features of active and reactive power, developed torque and speed of rotation. So, the GSC controls DC bus voltage and factor grid.

Unfortunately, connected to the grid, wind turbine is affected by numerous faults occurring in electrical power networks. In fact, during their operation, the DFIG can be exposed to difficult conditions or manufacturing defects [4, 5]. Its failure immediately paralyzes electricity production and can lead to a loss of wind system. So, to reduce damage, defects must be predicted in time.

This paper presents method developed for diagnosis defects attacking wind turbine doubly-fed induction generator. This method is based on analysis of frequency spectrum and Lissajous curves of DFIG stator and rotor currents. The approach is applied in the first place to a non-defected generator to have a reliable reference reflecting the behavior of DFIG wind turbine in healthy case. Afterwards, this diagnosis method is extended for defected asynchronous generator in order to predict in time the potential and imminent defects attacking wind turbine.

So, we start by the description of the wind turbine components. Then, we present the wind turbine modeling based on a mathematic model created in Matlab Simulink which reflects the behavior of the wind turbine. After that, we create a model of Doubly-Fed Induction Generator in which we applied an indirect field oriented control in order to increase performance of wind system. Afterwards, we propose a diagnosis defects method applied to wind turbine generator. This method is applied to defects-free generator and defected generator.

II. Wind Turbine Modeling

The Modeling of essential wind turbine components is based on the equations below [6]:

$$P_{wind} = \frac{\delta}{2}.A.v^3 \quad (1)$$

$$P_{turb} = \frac{\delta}{2}.A.C_p(\lambda,\beta).v^3 \quad (2)$$

$$C_p(\lambda,\beta) = k_1.(k_2.K - k_3.\beta - k_4).e^{-k_5 K} + k_6.\lambda \quad (3)$$

$$K = \frac{1}{\lambda + k_7.\beta} - \frac{k_8}{1+\beta^3} \quad (4)$$

$$\lambda = \frac{W_{turb}.R}{v} \quad (5)$$

$$T_{turb} = \frac{P_{turb}}{W_{turb}} = \frac{\delta}{2}.A.C_p(\lambda,\beta).v^3.\frac{1}{W_{turb}} \quad (6)$$

$$J = \frac{J_{turb}}{G^2} + J_g \quad (7)$$

$$J\frac{dW_{mec}}{dt} = T_g - T_{em} - f.W_{mec} \quad (8)$$

In order to have β =0 for a maximum Cp we take these values of the coefficients: k1= 0.5872, k2=116, k3=0.4, k4=5, k5= 21, k6= 0.0085, k7=0.08, k8=0.035 [7].

TABLE I
SYMBOLS AND ABBREVIATIONS USED IN WIND TURBINE MODELING

Symbol	Quantity
Pwind	Power of the wind
δ	Density of the air
A	Sweep area swept by the blade
v	Wind speed
$Pturb$	Power captured by the blade
$C_p(\lambda,\beta)$	Coefficient of performance
λ	Tip-speed ratio
$Wturb$	Angular speed of blade
β	Pitch angle (β =0 for maximum C_p)
$Tturb$	Torque of the blade
J	Inertia of the system brought back on the fast axis of turbine
J_{turb}	Turbine inertia
G	Gearbox ratio
J_g	Generator inertia
$Wmec$	Mechanical speed of DFIG
Tg	Aerodynamic torque on the fast axis of the turbine
Tem	Electric torque
f	Friction coefficient

The graphs below represent the simulation of the wind turbine model based on the mathematical equations in Matlab Simulink at the first thirty seconds. We suppose that the frictions are neglected. In fact, figure 1 represents the variable wind speed which we apply to wind system conversion.
The figures 2, 3, 4, 5 and 6 show the system performance. Actually,the wind power follows the same pace of wind speed (equation 1). The tip speed ratio is almost constant: it hardly changes values and equal to the optimal values. The coefficient of performance reaches its maximum value which is 0.56.

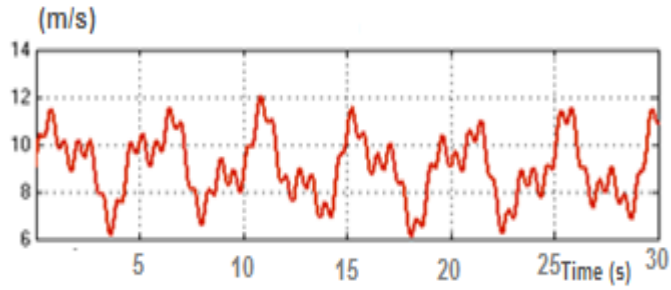

Fig. 1. Wind speed (m/s).

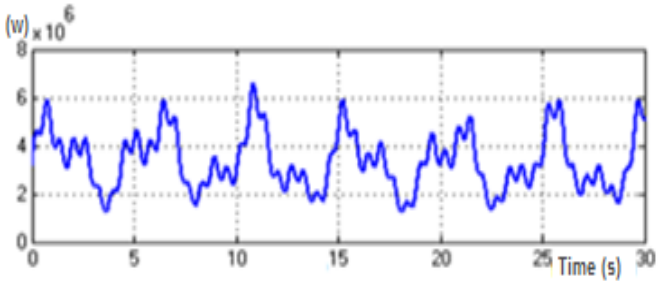

Fig. 2. Wind power Pwind (w).

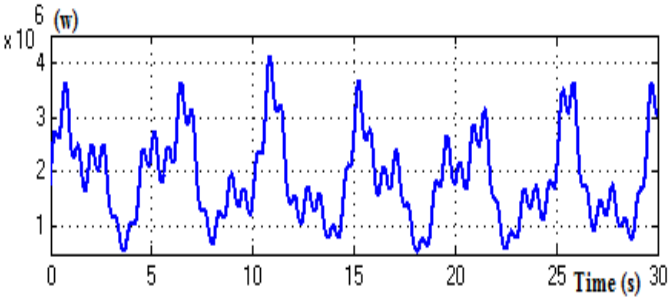

Fig. 3. Power captured by the blade Pturb (w).

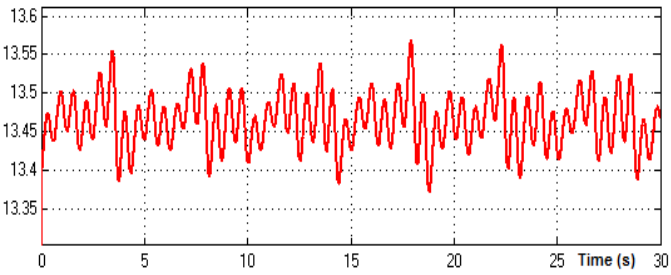

Fig. 4. Tip-speed ratio λ .

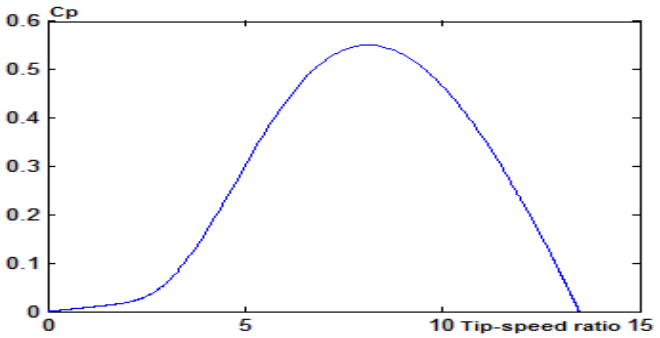

Fig. 5. Cp: Tip-speed ratio at β =0.

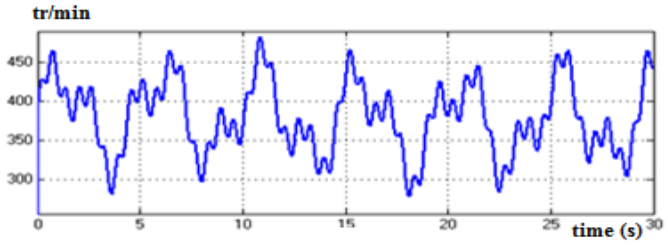

Fig. 6. Mechanical speed of DFIG.

III. DFIG MODELING

The equations for the stator voltages Us and the rotor Ur of DFIG in Park reference (d, q) are [8]:

$$\begin{cases} U_{ds} = \dfrac{d\phi_{ds}}{dt} + R_s.i_{ds} - \phi_{qs}\omega_s \\ U_{qs} = \dfrac{d\phi_{qs}}{dt} + R_s.i_{qs} + \phi_{ds}\omega_s \\ U_{dr} = \dfrac{d\phi_{dr}}{dt} + R_r.i_{dr} - \phi_{qr}(\omega_s - \omega_r) \\ U_{qr} = \dfrac{d\phi_{qr}}{dt} + R_r.i_{qr} + \phi_{dr}(\omega_s - \omega_r) \end{cases} \quad (9)$$

With: $\omega_r = \omega_s - P.w$ (10)

The flux equations can be written as follows:

$$\begin{cases} \phi_{ds} = L_s.i_{ds} + M.i_{dr} \\ \phi_{qs} = L_s.i_{qs} + M.i_{qr} \\ \phi_{dr} = L_r.i_{dr} + M.i_{ds} \\ \phi_{qr} = L_r.i_{qr} + M.i_{qs} \end{cases} \quad (11)$$

$$L_s = l_s - M_s, \qquad L_r = l_r - M_r$$

The electromagnetic torque expression will be:

$$T_{em} = p(\phi_{ds}.i_{qs} - \phi_{qs}.i_{ds}) \quad (12)$$

Where p represent number of pole pairs of the DFIG.

IV. FIELD ORIENTED CONTROL APPLIED TO DFIG

The aim of control by stator field oriented is to perform the control of active and reactive power of the DFIG by controlling dynamically and separately flux and torque. That is mean to orient stator flux along the direct axe to obtain:

$\phi_{qs} = 0$ and $\phi_s = \phi_{sd}$.

From equation (11) and equation (12) we get:

$$\begin{cases} i_{ds} = \dfrac{1}{Ls}(\phi_s - M.i_{dr}) \\ i_{qs} = -\dfrac{M}{Ls}.i_{qr} \\ T_{em} = p\phi_s.i_{qs} = -p\dfrac{M}{Ls}\phi_s.i_{qr} \end{cases} \quad (13)$$

In general, the stator resistance is negligible for large power equipment used in wind turbine. Also, it is supposed that the grid is stable and the field is constant. Thus, by replacing in equation (9) we have:

$$\begin{cases} U_{ds} = 0 \\ U_{qs} = \phi_s\omega_s \end{cases} \quad (14)$$

The active and reactive powers stator and rotor of DFIG can be written as follows:

$$\begin{cases} P_s = U_{ds}.i_{ds} + U_{qs}.i_{qs} \\ Q_s = U_{qs}.i_{ds} - U_{ds}.i_{qs} \end{cases} \quad (15)$$

We get the following expression of the active and reactive powers:

$$\begin{cases} P_s = -U_s\dfrac{M}{Ls}.i_{qr} \\ Q_s = \dfrac{U^2{}_s}{\omega_s.L_s} - U_s\dfrac{M}{Ls}.i_{dr} \end{cases} \quad (16)$$

So, the control of the active power is independent of the reactive power. Indeed, the active power is controlled by the quadrature rotor current iqr whereas the reactive power is controlled by the direct rotor current idr.

$$\begin{cases} U_{dr} = (R_r + S(L_r - \dfrac{M^2}{Ls})).i_{dr} - g\omega_s(L_r - \dfrac{M^2}{Ls}).i_{qr} \\ U_{qr} = (R_r + S(L_r - \dfrac{M^2}{Ls})).i_{qr} + g\omega_s(L_r - \dfrac{M^2}{Ls}).i_{qr} + g\dfrac{M}{Ls}.U_s \end{cases} \quad (17)$$

TABLE II

SYMBOLS AND ABBREVIATIONS USED IN DFIG MODELING

Symbol	Quantity
ϕ_s (d, q)	Stator field in Park reference
ϕ_r (d, q)	Rotor field in Park reference
Rs	Stator resistance
Rr	Rotor resistance
Ls	Cyclic inductances of stator
Lr	Cyclic inductances of rotor
ls	Leakage inductances of stator
lr	Leakage inductances of rotor
Ms, Mr	Respectively mutual inductances between stator and rotor phases
M	Maximum mutual inductance between stator and rotor stage (the axes of the two phases coincide)
i_s (d,q)	Stator current in Park reference
i_r (d,q)	Rotor current in Park reference
Tem	electromagnetic torque
U_s (d,q)	Stator voltage in Park reference
Ur (d,q)	Rotor voltage in Park reference
P_s	Active power of DFIG
Q_s	Reactive power of DFIG

The vector control is divided in two approaches: direct and indirect. The direct one is simple to implement but not the most efficient [9], [10], [11]. The indirect method is being more commonly used [12], because it allows us to operate more easily throughout all the speed range [13].

In this paper the wind turbine model has been implemented in Matlab Simulink and the simulations are done with the indirect vector field oriented control. The simulation results are summarized in following figures.

In DFIG modeling, we chose to orient the stator flux of DFIG according to the direct axe. The simulation results are presented in the figure 7. It is shown that the indirect flux values of stator machine reached to zero.

The direct stator flux is constant as illustrated in figure 8.

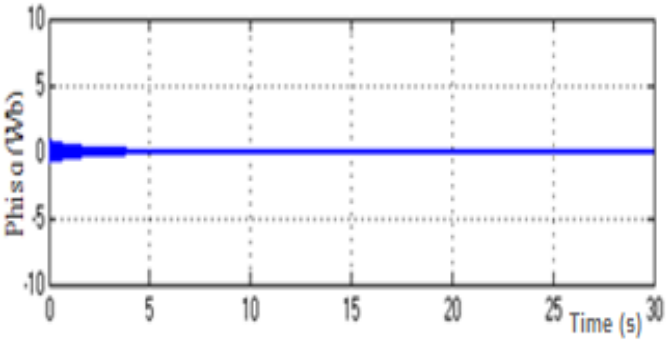

Fig. 7. Indirect stator field of DFIG.

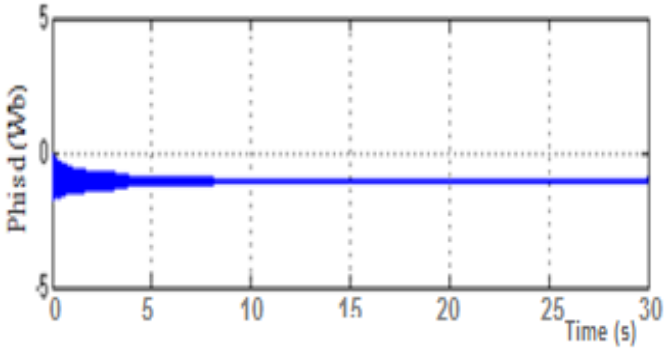

Fig. 8.Direct stator field of DFIG.

In addition, a reference for active power Psref is chosen to have a form of three steps applied in different time. Indeed the first step is applied at the start time. At 0.3 second, another step is added to the first step. The third step is applied after one second. As illustrated in figure 9, the active power follows the reference Psref.

Also, the system reactive power is also around the reactive power reference which is zero as shown in figure 10.

Figures 11 and 12 present variations of the direct and quadrature stator currents (ids, iqs) and rotor currents (idr, iqr).

The simulations showed that the active power is controlled by the quadrature rotor current iqr. The reactive power is controlled by direct rotor current idr (equation 16).

So, the coupling between the two powers is barely perceptible.

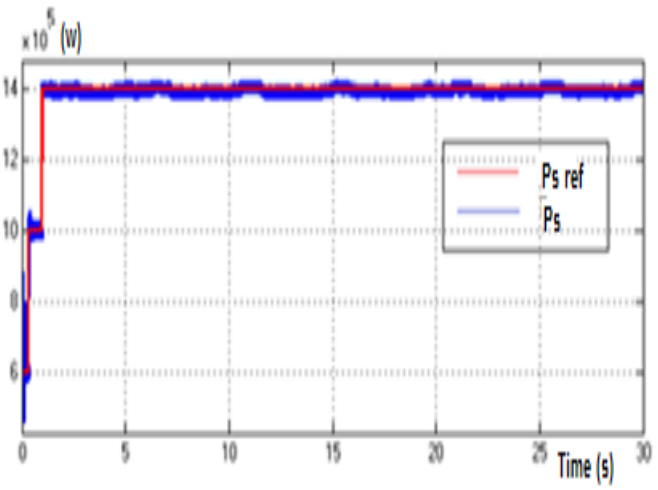

Fig. 9. Comparison between Psref and Ps.

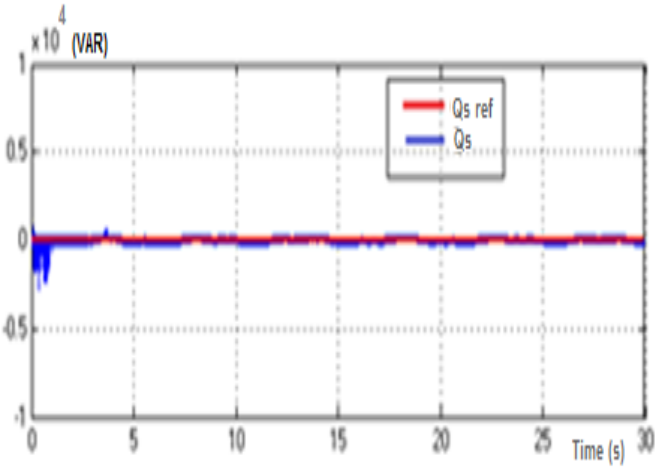

Fig. 10. Comparison between Qsref and Qs.

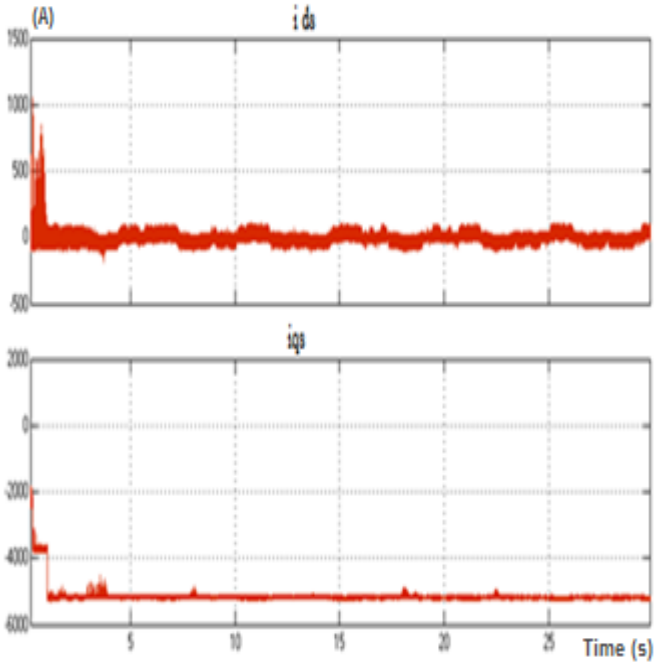

Fig. 11. Direct and indirect DFIG stator currents.

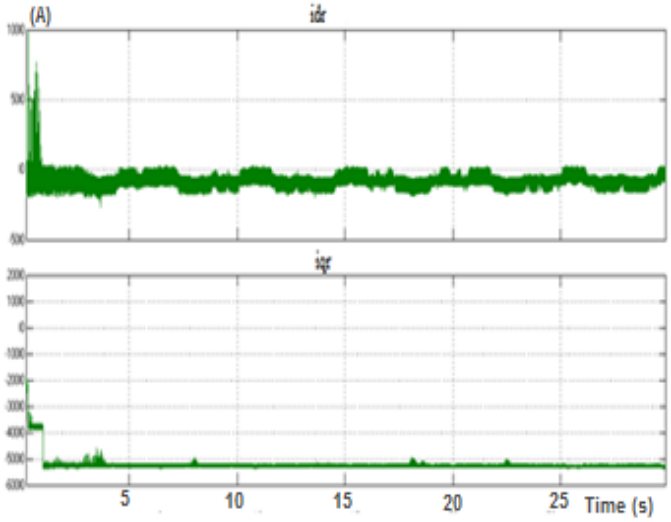

Fig. 12. Direct and indirect DFIG rotor currents.

A zoom on doubly-fed Asynchronous generator three-phase stator currents is presented in figure 13. It is shown that DFIG three-phase stator currents isabc have perfect sinusoidal shapes.

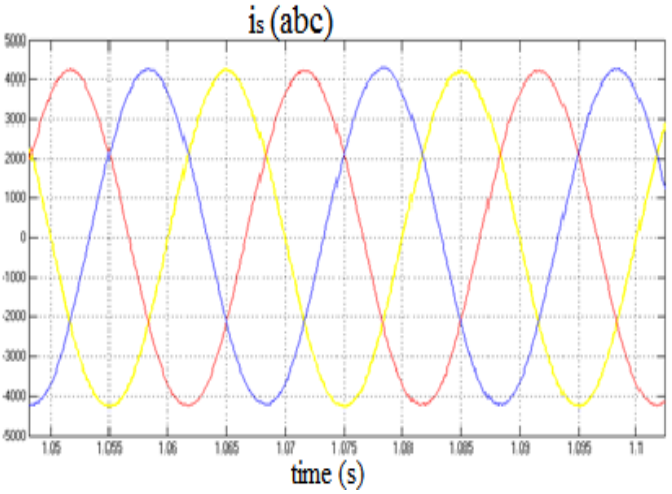

Fig. 13. Three phase stator currents.

All these figures introduced show performance of our wind system model created in the Matlab Simulink.

V. Grid And Wind Turbine

By the last decades, penetration of wind energy on the grid is in rise. Indeed, wind power is the most competitive option for the growing electricity demand. It could supply up to 20% of global electricity by 2030 [14].

In fact, wind energy power is injected in medium voltage and high-voltage network of the utility. In this situation, grid operators need to ensure that the electric power system operates continuously in a safe and economic way [15].

However, faults in electrical power networks are inevitable and unpredictable events. They can be temporary or permanent. Temporary fault disappears after the action of protective devices. But permanent fault requires isolation of equipment and reparation by operators.

As, wind turbine is connected to grid, the wind structure is consequently subjected to grid faults.

Indeed, Wind turbines, connected to the grid are exposed to various grid faults. We mentioned lack or variation of the voltage grid magnitude and frequency and short circuit in the grid. These grid faults lead to an overheated generator and over-current in generator stator phases [16].

Moreover, according to study and analyses defects of Moroccan wind turbine park, percentage of wind turbine defects due to only grid faults represents 22% of all defects attacking park during one year [17]. This percentage is the highest after electrical defects as illustrated in figure 14.

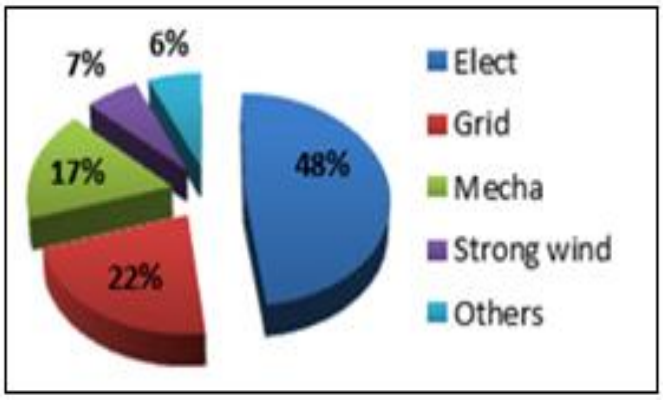

Fig. 14. Defect types in Moroccan wind turbine park.

Various grid faults can occurs in electrical networks and the most common grid fault is short-circuits fault [18]. They may be generated by temperature rise, partial discharge and accidental electrical connection between two conductors [19].

The short-circuit currents cause excessive heating which can lead to fire, explosion and probably the complete loss of the power system elements. That is why, grid operators used the short-circuit current to define electrical grid elements specifications and to select appropriate setting for protection system.

Another fault related with the network is unbalanced voltages. Unbalanced voltages are unequal voltage values on three phase circuits. These voltages may differ by a few volts. But when difference voltages are excessive problems occur and can cause serious damages to inductive devices especially motors [20]. Usually, the unequal voltage values are due to variations in the load which are caused for example by unbalanced incoming utility supply, unequal impedance in conductors of power supply wiring, open phase on the primary of three phase transformer on the distribution system etc.

When fault occurs in the grid wind turbine is disconnected in order to avoid loss structure; however, for large wind energy capacity disconnection from the grid could generate problems in the control of frequency and voltage in the system [21].

For this reason, it is necessary to diagnose wind turbine doubly-fed induction generator (DFIG) when a grid fault was detected.

VI. DFIG DIAGNOSIS DEFECTS

Many research papers deal with different methods for wind turbine diagnosis defects to save both money and time in wind power generation system [22]. For monitoring and supervising the wind conversion system health some techniques use time-frequency analysis tools such as wavelets to derive a fault detection signal [23]. Also, methods of process simulation and construction of algorithm are used in condition monitoring to detect and anticipate defects [24].

Some methods are exploring data provided by the supervisory system and apply many data-mining algorithms to develop models for predicting occurrence of possible defects [25]. These different techniques are widely used in control system for reducing the down time of the wind turbine and minimizing operational and maintenance costs.

A. Method Applied to Generator During Defects-Free Operation

We develop technique for DFIG diagnosis defects based on frequency spectrum analysis and stator and rotor currents Lissajous curves.

This method is applied to generator during defects-free operation to obtain a reliable reference for behavior of doubly-fed induction generator.

We start by applying Fast Fourier Transform FFT to three-phase stator currents, which is a transformation commonly used in digital signal processing. It allows conversion of a signal from its original domain to a representation in the frequency domain.

FFT analysis was used to determine the amplitude of the harmonic components and to find the maximum amplitude spectrum of the wavelet coefficients [26].

Indeed, the analysis of stator current and rotor current in the spectral field offers a source of defects information thanks to the resulting spectrum [27].

The FFT analysis of the stator three-phase currents and harmonic spectra was implemented as shown in figure 15.

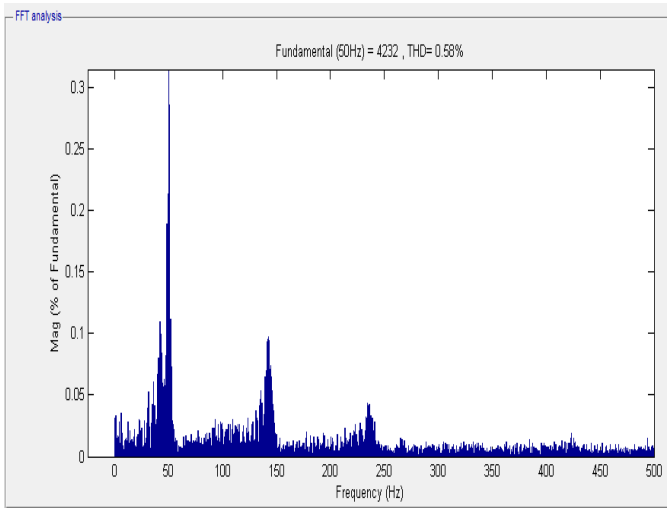

Fig. 15. Fast Fourier Transformer spectrum of stator currents.

The fundamental frequency is at 50 Hz and the Total Harmonic Distortion (THD) is equal to 0.58%.

In addition, due to the use of Pulse Width Modulation (PWM) in the system, harmonics are detected at frequency equals to 150 Hz and at 250 Hz. they represent the third and fifth harmonics. Also, magnitude percentages are respectively 0.1% and 0.05%.

Furthermore, Lissajous curves are applied in this paper to the DFIG stator and rotor three-phase currents.

The figures 16 and 17 below illustrate Lissajous curves in case of generator under normal operating condition.

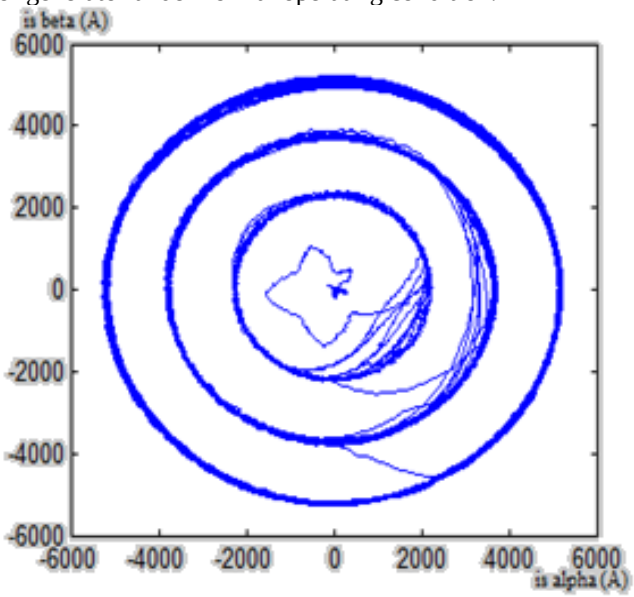

Fig. 16. Lissajous curves of DFIG stator currents.

In case of non-defected generator, figure 16 shows Lissajous curves of DFIG stator curents. Actually, Lissajous curves have three circular shapes passing from the small circle to the biggest one. These circles are due to Psref. actualy, as shown in figure 9, Psref is chosen as a signal with three steps shape.

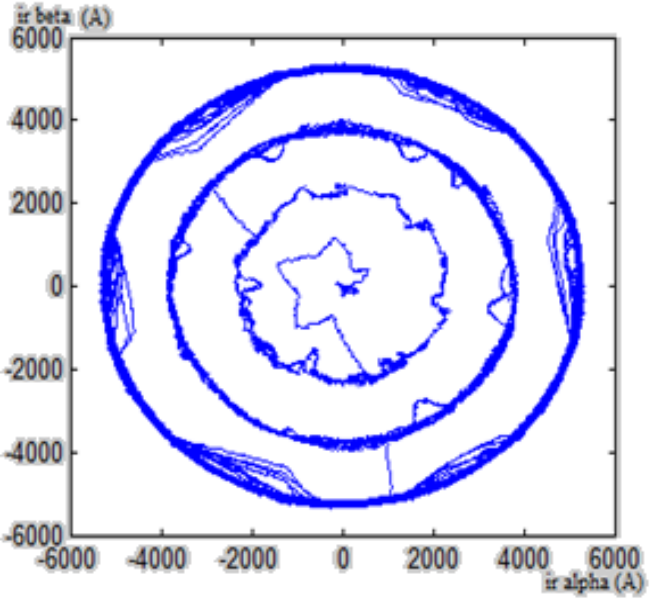

Fig. 17. Lissajous curves of DFIG rotor currents.

The figures 17 shows DFIG rotor currents Lissajous curves case of non-defected generator. The rotor curents Lissajous curves have a 6 petals flower shape. This shape is due to the DFIG rotor supply by the inverter with 6 switches. Also, like stator, rotor curents Lissajous curves have three circular shapes because of Psref three steps signal.

B. Method Applied in Case of Defected Generator

In this part we apply diagnosis method to defected wind turbine double-fed induction generator. As mentioned in previous paragraph, grid faults are unfortunately inevitable and unpredictable events. As a wind turbine is connected to the grid, the system is immediately exposed to various grid faults.

Considering complexity and diversity of grid defects attacking wind energy system, we chose in this paper to deal with lack and unbalanced voltages with variation of the magnitude and frequency.

1) Case of Va= 0

Firstly, a diagnosis method is applied in case of one grid voltage phases luck.

The figure 18 below represents Fast Fourier transformer spectrum FFT of stator currents in case of generator fed from two phase power supply.

We not that, in addition to harmonics at frequency equals to 150 Hz and at 250 Hz (case of defects-free generator), peaks appear in new frequency (at 25 Hz and 75 Hz).

Also, Total Harmonic Distortion THD passed from 0.58% in normal operating condition of generator to 24.07% in case of defected generator.

Indeed, higher THD means increase of generator heating and peak currents. As showed in figure 15 fundamental magnitude was 0.31%. But, when Va= 0, this fundamental magnitude value passed to 24%.

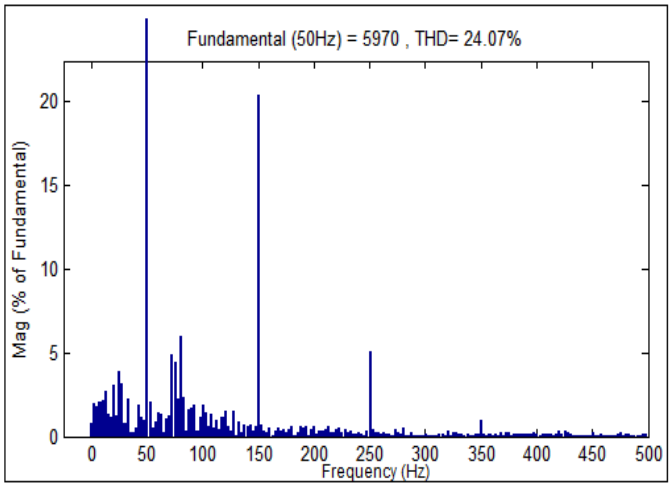

Fig. 18. Fast Fourier Transformer spectrum of stator currents.

Moreover, comparing stator and rotor Lissajous curves obtained in case of defected generator to normal operating condition of generator Lissajous curves, we see clearly in figures 19 and 20 that stator and rotor curves are deformed.

Indeed, Lissajous curves of DFIG stator currents are not any more in circular shapes. The curves have now elliptical shapes. Also thickness increases, which makes difficult observation of three separate curves due to three steps of Psref.

It is noted that, the circumference of stator Lissajous curves is increased as shown in figure 19.

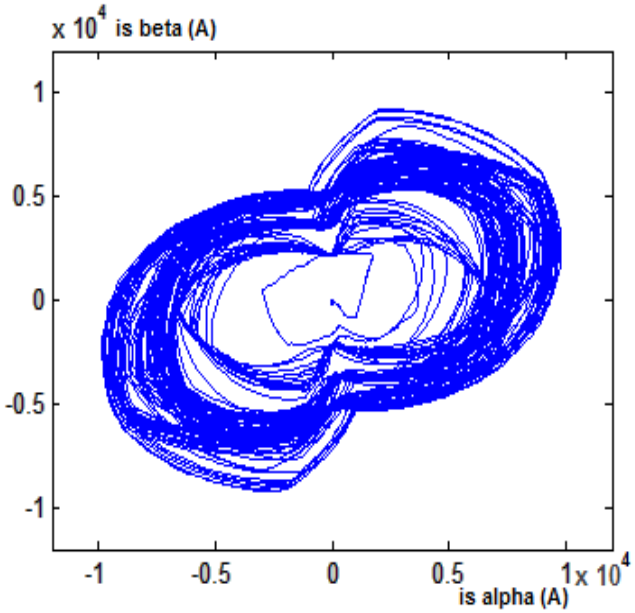

Fig. 19. Lissajous curves of DFIG stator currents.

For DFIG rotor currents Lissajous curves shown in figure 20, we can not separat three curves. They are superimposed on each other because of increasing curves thickness.

Also, the figure 20 shows a six petals flower shape but it is defomed comparing to the reference curves in case of asynchronous generator under normal operating condition .

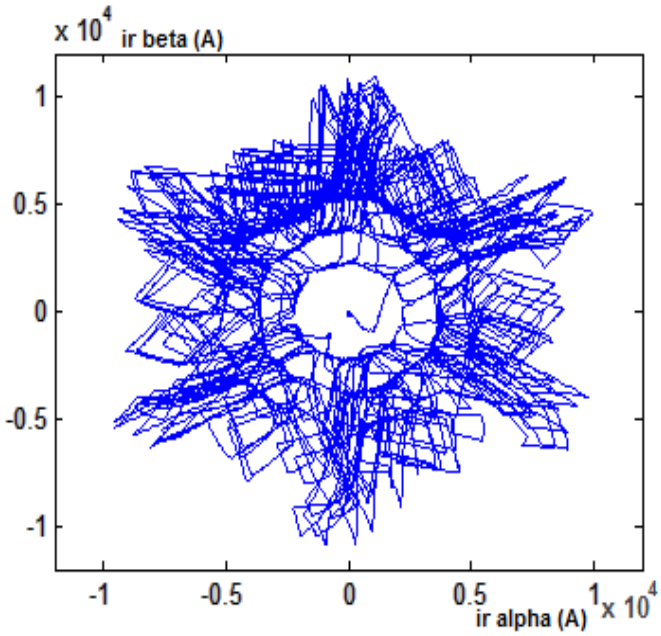

Fig. 20. Lissajous curves of DFIG rotor currents.

2) Case of unbalanced voltages with various amplitudes

Perfectly voltage-balanced cannot exist in power distribution system. Actually, when voltages differ excessively they may cause damage to wind turbine doubly-fed induction generator. In this paragraph we deal with unbalanced voltages and we use various amplitudes of three phase voltages stator power supply.

The figure 21 illustrates Fast Fourier Transformer spectrum FFT of stator currents in case of unbalanced voltages with different amplitudes.

We note that Total Harmonic Distortion THD passed from 0.58% in normal operating condition of generator to 14.93% in case of defected generator.

Moreover, as generator is under abnormal condition operating (unbalanced voltages), the currents signal amplitude increases. Indeed, the magnitude of fundamental passed to 17% instead of 0.1% (case of generator under normal operating condition). Besides, the third and the fifth harmonics respectively at 150Hz and 250 Hz continue to occur due to the use of PWM as mentioned previously. But in the case of defected generator, the third and the fifth harmonics magnitudes are greatly increased.

Actually, compared to DFIG stator currents FFT in figure 15, the magnitude of the third harmonic passed from 0.1% to 14%. Also we noted that the fifth harmonic magnitude passed from 0.05% to 2%.

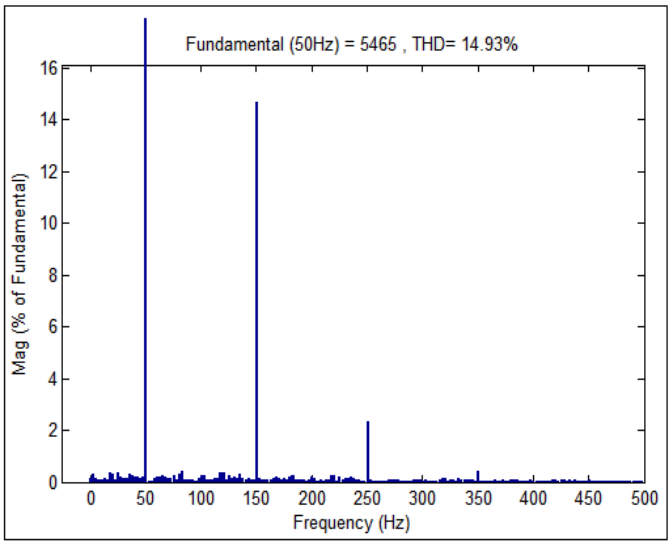

Fig. 21. Fast Fourier Transformer spectrum of stator currents.

The following figures 22 and 23 show Lissajous curves of respectively generator stator and rotor currents in case of unbalanced voltages (amplitude variation).

In these figures we can observe deformation of Lissajous stator and rotor curves.

In fact, as showed in figure 22, stator currents Lissajous curves became ellipses. These three separate oval shapes are due to Psref. Also, we can observe that curves thickness incresed when unbalanced voltages occur.

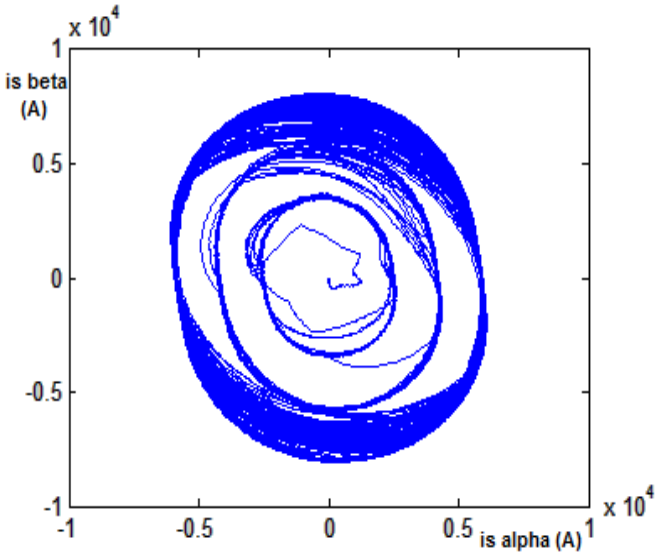

Fig. 22. Lissajous curves of DFIG stator currents.

The same for rotor currents Lissajous curves, the thickness increases in case of unbalanced voltages (amplitude variation). In addition, the rotor curves are superimposed which makes a six petals flower shape hard to distinguish.

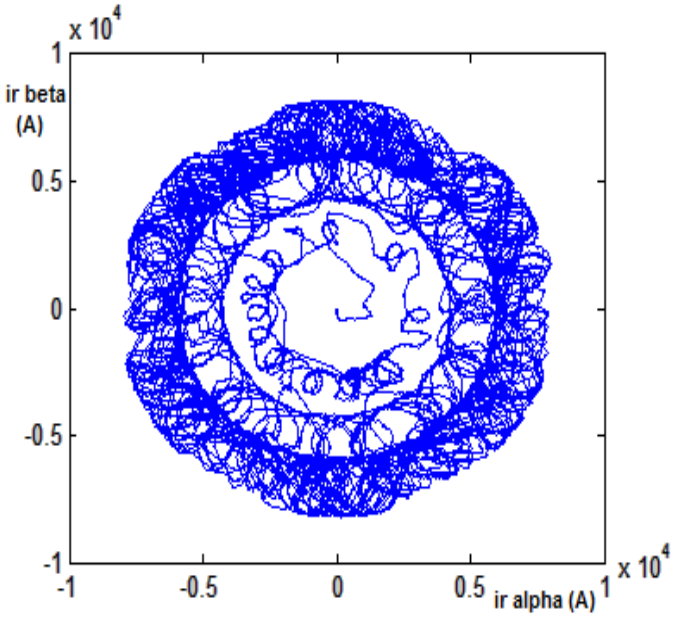

Fig. 23. Lissajous curves of DFIG rotor currents.

3) Case of unbalanced voltages with various phases

The figure below represents Fast Fourier transformer spectrum FFT of stator currents in case of unbalanced voltages with various phases.

In this case, some considerable currents peaks appear in new frequency for example at 0 Hz, 25 Hz, 75 Hz and 100 Hz with less than 3% in magnitude.

Furthermore, Total Harmonic Distortion THD value reaches to 22.24%. This is far from THD value in normal operating condition of generator (0.58%).

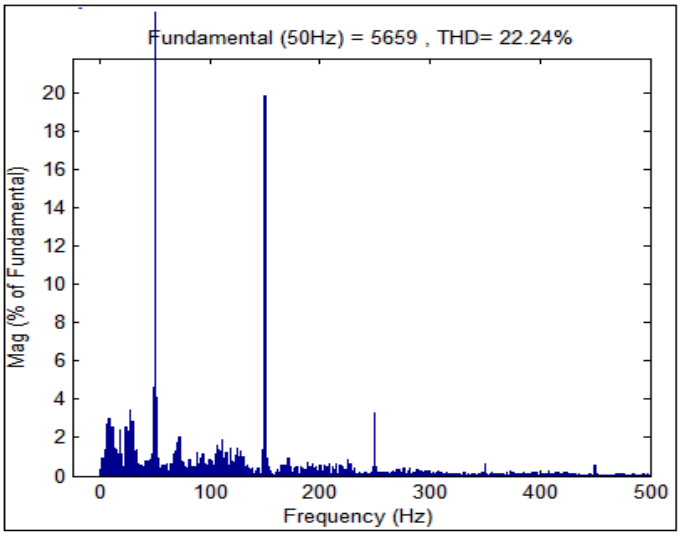

Fig. 24. Fast Fourier Transformer spectrum of stator currents.

In case of unbalanced voltages with various phases, Lissajous curves of DFIG stator currents are deformed. The curves have in this case elliptical shapes.
Also the circumference and thickness of stator Lissajous curves increased as shown in figure 25.
In addition, the stator curves are superimposed and make difficult observation of three separate curves due to three steps of Psref as in normal operationg condition of generator.

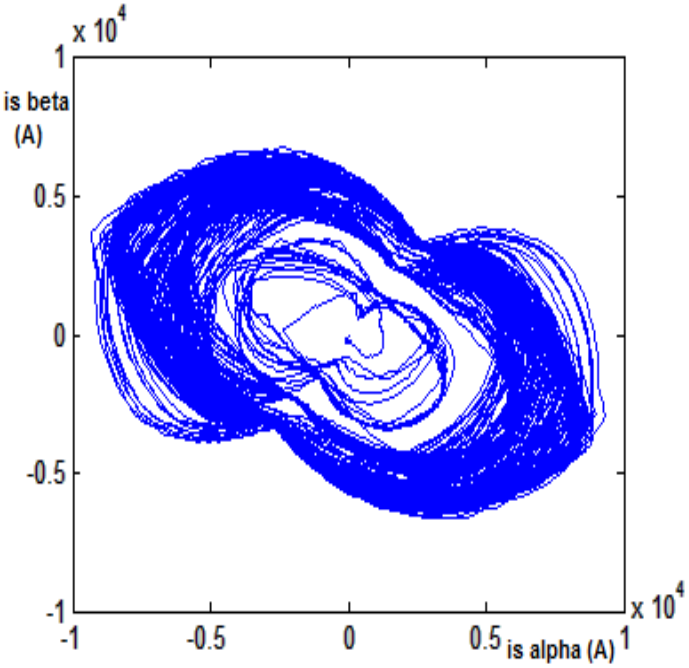

Fig. 25. Lissajous curves of DFIG stator currents.

In figure 26, DFIG rotor currents Lissajous curves are exposed. It is obseved that due to increasing thickness, the curves are superimposed on each other.
Also, the curves have a shape of six petals flower. However, it is defomed comparing to the case of asynchronous generator under normal operating condition.

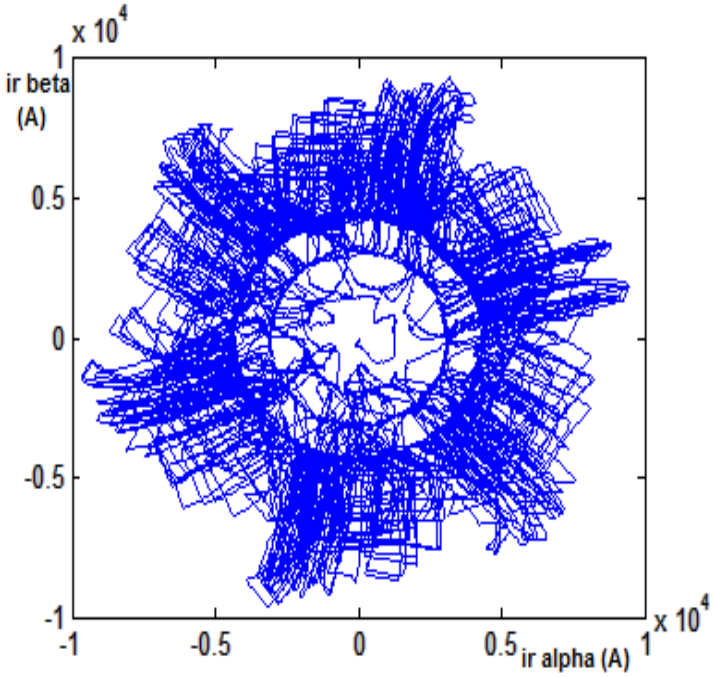

Fig. 26. Lissajous curves of DFIG rotor currents.

VII. Conclusion

In this article we introduce method to diagnose wind turbine doubly-fed induction generator defects.

We start by modeling wind energy system created in Matlab Simulink basing on mathematic equations. Then, the field oriented control was applied to control dynamically and separately flux and torque, which allows an independent control of active and reactive power of the DFIG. In addition, the indirect vector control was applied with the aim of having efficient, easy and optimal operation of electrical generation system throughout all the speed range.

Then, method was developed to predict the potential defects through studying frequency spectrum analysis and Lissajous curves. This method is applied in case of abnormal condition operating of generator and compared with reference results obtained in case of defect-free operation. In this paper, we deal with lack and unbalanced voltages (variation of the magnitude and frequency). Indeed, using FFT analysis peaks appear at new frequencies in the presence of defects. The peaks amplitude, give us an idea about the severity of the defects attacking the system. Also, stator and rotor currents Lissajous curves are deformed according to defects types. This gives us an idea about the kind of the defects attacking wind conversion system generator. The simulations had been realized by Matlab Simulink. These results showed the efficiency of the proposed method in DFIG diagnosis defects.

The future work will be about modeling and simulating other defects such as short-circuits and voltage dips. Then, application and validation of diagnosis method in presence of these defects.

REFERENCES

[1] A speech of His Majesty the King Mohamed VI of Morocco, *COP22* in Marrakech, November 2016.

[2] R. M. R. Muthu, "Doubly Fed Induction Generator for Wind Energy Conversion System - a Survey", *International Conference on Energy Efficient Technologies for Sustainability*, pp. 617-628, 2013.

[3] M. A. El-Sharkawi, "Wind Energy An introduction", *University of Washington*, Seattle, USA: 219, 2016.

[4] S. Martens et al., "Simulation of Electric Faults in Doubly-Fed Induction Generators Employing Advanced Mathematical Modeling", *Proceedings of 24th Nordic Insulation Symposium on Materials, Components and Diagnostic*, pp.98-104, 2015.

[5] A. Joshuva and V. Sugumaran, "Fault Diagnostic Methods for Wind Turbine: A Review", *Journal of Engineering and Applied Sciences (ARPN)*, vol. 11, no 7, pp. 4654-4668, 2016.

[6] Y. Amirata, et al., "A brief status on condition monitoring and fault diagnosis in wind energy conversion system", *Renewable and Sustainable Energy* Reviews, vol. 13, issue 9, pp. 2629–2636, 2009.

[7] B. Bossoufi, et al., "Observer backstepping control of DFIG-Generators for wind turbines variable-speed: FPGA-based implementation", *Renewable Energy*, vol.81, pp. 903-917,2015.

[8] A. Boyette, "Contrôle-commande d'un générateur asynchrone à double alimentation avec système de stockage pour la production éolienne", *thèse doctorat. Université Henri Poincaré*, Nancy I, 2006.

[9] Y. Ihedrane, et al., "Power Control of DFIG-Generators for Wind Turbines Variable-Speed", *International Journal of Power Electronics and Drive System (IJPEDS)*, vol. 8, no. 1, pp. 444-453,2017.

[10] M. Allam, et al., "Etude comparative entre la commande vectorielle directe et indirecte de la Machine Asynchrone à Double Alimentation (MADA) dédiée à une application éolienne", *Journal of Advanced Research in Science and Technology*, vol/issue: 1(2), pp. 88-100, 2014.

[11] B. Bossoufi, et al., "FPGA-Based Implementation nonlinear backstepping control of a PMSM Drive", *IJPEDS International Journal of Power Electronics and Drive System*, vol. 4, issue: 1, pp. 12-23, 2014.

[12] K. Sejir, "Commande Vectorielle d'une Machine Asynchrone Doublement Alimentée (MADA)", *Thèse de Doctorat de l'Institut National Polytechnique de Toulouse*, France, 2006.

[13] Gan Dong," Sensorless and Efficiency Optimized Induction Machine Control with Associated Converter PWM Modulation Schemes", *The Faculty of the Graduate School*, Tennessee Technological University, 2005.

[14] Biennial Global Wind Energy report from Global Wind Energy Council GWEC, *The Actuary The magazine of the Institute & Faculty of Actuaries*, October 2016.

[15] K. Loudiyi, et al., "Grid code status for wind farms interconnection in Northern Africa and Spain: Descriptions and recommendations for Northern Africa", *Renewable and Sustainable Energy Reviews*, Elsevier, vol. 81, part 2, pp. 2584-2598, 2018.

[16] F. El Hammouchi, L. El Menzhi and A. Saad, "Wind Turbine Doubly-Fed Asynchronous Machine Diagnosis Defects-State of the Art", *DEStech Transactions on Environment Energy and Earth Sciences*, pp. 300-306, October 2017.

[17] F. El Hammouchi, et al., "Wind Turbine Double-fed Asynchronous Machine Diagnosis Defects-Part One", *International Congress of Industrial Engineering and Systems Management CIGIMS*, Meknes, Morocco, pp. 380-383, Mai 2017.

[18] V. Chetty, "Network Studies and Mitigation of High 132 Kv Fault Currents in Ethekwini Electricity", *thesis report*, South Africa College of Agriculture, Engineering and Science Discipline of Electrical, Electronic and Computer Engineering, December 2016.

[19] A. A. Sallam and O. P. Malik, "Electric Distribution Systems", *Collection IEEE Press Series on Power Engineering*, 2nd edition, 624 pages, pp. 111-121, 2018.

[20] M. A. Sheikh, et al., "An Analytical and Experimental Approach to Diagnose Unbalanced Voltage Supply", *Arabian Journal for Science and Engineering*, vol. 43, issue 6, pp. 2735–2746, June 2018.

[21] Hansen, et al., "Grid Fault and Design-Basis for Wind Turbines - Final Report", *Roskilde, Risø National laboratoriet for Bæredygtig Energi*, Denmark, Forsknings center Risoe. Risoe-R, no. 1714, 2010.

[22] A. Joshuva and V. Sugumaran,"Fault Diagnostic Methods For Wind Turbine: A Review", *ARPN Journal of Engineering and Applied Sciences*, vol. 11, no. 7, pp. 4654-4668, 2016.

[23] W. Yang, P. J. Tavner, C. J. Crabtree and M. Wilkinson, "Cost-Effective Condition Monitoring for Wind Turbines", *IEEE Transactions On Industrial Electronics*, vol. 57, no.1, 2010.

[24] S. M. Tabatabaeipour, et al., "Fault Detection of Wind Turbines with Uncertain Parameters: A Set-Membership Approach", *Energies*, vol. 5, pp. 2424-2448; doi: 10.3390/en5072424, 2012.

[25] A. Kusiak, W. Li, "The Prediction and Diagnosis of Wind Turbine Faults", *Renewable Energy*, vol. 36, issue 1, pp. 16-23, 2011.

[26] F. El Hammouchi, L. El Menzhi, A. Saad, Y. Ihedrane, B. Bossoufi, "Wind Turbine Doubly-Fed Asynchronous Machine Diagnosis Defects-part two", *Congress CIST 18 Conference OMCS, IEEE XPLORE catalogue number* CFP1867R-ART, pp. 486-454, 2018.

[27] E. ElBouchikhia, et al., "Induction machine faults detection using stator current parametric spectral estimation", *Mechanical Systems and Signal Processing*, vol. 52–53, pp. 447-464, February 2015.

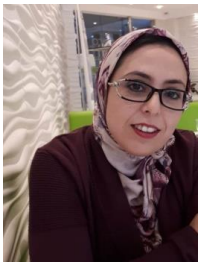

F. El Hammouchi was born in Morocco on October 16th, 1985. In 2008, she received the Engineer degree in Electrical Engineering and Power Electronics (EEP) from the National Higher School of Electricity and Mechanics (ENSEM) Hassan 2 University of Morocco in Casablanca.

Fatima is PhD student in electrical engineering at Electrical Systems Team (EST) of ENSEM since 2015. She is interested in electrical machines modeling, control, on line diagnosis defects in wind turbines, and their integration in grid.

L. El Menzhi is a professor in Abdelamalek Essaadi University in Morocco since 2010. On 2002, she got her High Deepened Studies Diploma in electrical machines in electrical engineering from the High National School of Electricity and Mechanics ENSEM in Hassan 2 University in Casablanca.

On 2009, Lamiaa obtained her Doctor degree, then her Habilitation as a professor researcher on 2016 from Hassan 2 University in Casablanca (ESEM). She is interested in electrical machines control and on-line diagnosis either used as a motor or a generator in wind turbines. She is a member and advisor of the Moroccan Center of Polytechnical Research and Innovation since 2015.

A. Saad was born in Morocco in September 1956. He received the Engineer and Doctor of Engineering degrees from National Polytechnic Institute of Grenoble – France – respectively in 1980 and 1982. From 1982 to 1986, he was Researcher at French National Center for Scientific Research (CNRS) - Electrostatics and Dielectric Materials Laboratory – Grenoble.

After receiving the Doctor of Physical Sciences degree in 1986, Abdallah joined Hassan 2 University of Morocco. Professor of electrical engineering, he has several scientific and educational responsibilities. His main fields of interest are High Voltage and Electrical Insulations, modeling and control, renewable energy integration.